

When Renewable Energy Meets Building Thermal Mass: A Real-time Load Management Scheme

Yan Shen, Zhonghao Sun, and Qinglong Wang

Abstract

We consider the optimal power management in renewable driven smart building MicroGrid under noise corrupted conditions as a stochastic optimization problem. We first propose our user satisfaction and electricity consumption balanced (USECB) profit model as the objective for optimal power management. We then cast the problem in noise corrupted conditions into the class of expectation maximizing in stochastic optimization problem with convex constraints. For this task, we design a Bregmen projection based mirror decent algorithm as an approximation solution to our stochastic optimization problem. Convergence and upper-bound of our algorithm with proof are also provided in our paper. We then conduct a broad type of experiment in our simulation to test the justification of our model as well as the effectiveness of our algorithm.

I. INTRODUCTION

The concept of smart grid that incorporating power transmission system and end users in an integral system has been gradually embraced by independent system operators(ISO) [1]. Smart buildings utilizes the advancement of power electronics, communication technology [2] and control theory to allow for the dynamic interaction between power grid and end users without human intervention. The drivers for smart grid are not only the financial benefit for end users generated by energy consumption cost reduction but also the positive effect on grid operation stability. On the other perspective, smart building is considered as an ideal active participant of demand response program for its ability to regulate power consumption using its thermal mass capacities [3]. Deployed with advanced load control technology, smart building can smartly coordinate their power consumption with smart grids load condition [4]. However smart buildings power consumption pattern that copeaks with power grids load occupancy condition limits its

load regulating ability. Power systems stability condition will become fragile when buildings air-conditioning power suddenly increases in the condition of high volume load in power grid.

The northeast blackout of 2003 can be provided as a typical example of cascaded widespread power system failure triggered by surging building air conditioning loads in a hot summer. According to the technical analysis conducted by North American Electric Reliability Council [5], there is no matter that the stringent power consumption caused by high air-conditioning usage served as a catalyst to worsen the whole event, though the direct cause that triggers the power failure is the failing of the alarm and logging system in FirstEnergy control room [6].

This motivates us to find a substitutional approach to mitigate the impact of smart buildings overloading in peak hour. Thanks to the deregulation of electricity market and the advancement of MicroGrid technology, supplying smart building with local renewable generation through the interconnection of MicroGrid becomes a feasible solution to reduce smart buildings reliance on Grid. As renewable generation copeaks with the smart buildings power consumption (typically in a hot summer afternoon), local renewable can be efficiently utilized by smart buildings nearby without the need of long distance transmission. In this paper, we discuss the possibility of incorporating the smart building load and renewable generation together in a MicroGrid by studying the stability condition of power grid under load and generation fluctuation. Power management strategy is deployed in our MicroGrid to achieve the dual goal of minimizing outside power consumption and maximizing user satisfaction. Measurement error and renewable generation uncertainties are also considered in our paper.

The **main contribution** of this paper is three folds: In one perspective, we propose the concept of supplying smart building with local renewable energy as a complimentary power source to commercial grid. In another perspective, we develop our user satisfaction and electricity consumption balanced (USECB) profit model as a objective goal for power management strategy in MicroGrid. Our contribution is not only limited in system model but also in theory of algorithms, we design a Bregemen projection [7] based mirror decent algorithm as a stochastic optimization scheme with convergence analysis.

Our paper is organized as follows: In section(IV), we first introduce the back ground of power transmission network and applies the linear approximation model in our MicroGrid as system model. In section(V), we formulate our optimal power management problem in renewable driven smart building MicroGrid. In section(VI), we introduce our Bregemen Projection based mirror decent algorithm. In section(VII), we show the performance of our model and algorithm via

simulation. [8]

II. RELATED WORK

Up to now, many studies have proposed the concept of smart building's load control using its thermal mass capacities. P.Xu has studied smart building's load control potential in Public Interest Energy Research (PIER) Program that was conducted at the Santa Rosa Fedral Building. Field test were performed in two buildings [10]. The result of load monitoring together with comfort surveys concludes the potential to perform demand response in commercial buildings while maintaining acceptable comfort conditions. However these studies are performed in the framework of passively following grid's regulation signal while omitting the part of interactive influence by considering the actual power grid model. B.Ramanathan has incorporated the interactive influence part in power grid in their load control modeling. However they only use an empirical one from Nordic power system for a specific performance without universal applicability [9], [11], [12].

As generally studying the impact of smart building's load control in power grid need to adopt a concise and exact power grid model, DistFlow model [13] is among the most popular exact power grid model. However DistFlow model can not be directly applied because of the inconvex nature of the model. S.Low has developed a convex relaxation of DistFlow model [14], [15]. This model is effective in solving most of the optimal power flow (OPF) problem. Though the theoretical exactness is only proved in radical cases, simulation evidence has shown that its exactness can be broadly extended to general cases. S.Bolognani has generalized one DC power flow model to AC power grid systems. This model is developed by the first order Tyler approximation of power injection equations. High exactness for MicroGrid in grid connected case has been tested in simulations.

The concept and enabling technologies for the Customer-driven MicroGrid has been extensively studied in many researches. S.Suryanarayanan has surveyed the enabling technologies of the Customer-driven MicroGrid [16]. P. Dondi has reviewed the position of distributed generation with respect to the installation and interconnection of such units [17]. Actually many of these technologies have been applied to the MicroGrid testing systems. The concept of MicroGrid has gone beyond its seminar stage [18]. Actual onsite testbed has been installed as a precursor for later residential product. Consortium for Electric Reliability solution(CERTS) testbed has been experimented in Lawrence Berkeley lab campus [19]. Distributed renewable generation

resources [20] have been integrated in CERTS MicroGrid. Testing on MicroGrid components has also been extensively conducted by ISET in Germany. The More Project located at Bronsbergen Holiday Park, located near Zutphen in the Netherlands aims at the increasing penetration of microgeneration in electrical networks through the exploitation and extension of MicroGrid concept [21].

III. SUPPLYING SMART BUILDING WITH LOCAL RENEWABLES:MOTIVATIONS AND CHALLENGES

Despite of smart building's load control ability by using its thermal mass capacity, researches are mainly focused on adjusting its power consumption pattern to adapt to the peak and valley signals generated by conventional grid without noticing the fact that the peak and valley signals are generating by the grid according to the congestion conditions of its major transmission branch rather than the ability of its instantaneous generating capacities to meet its demands. As the distribution network of conventional commercial grid is typically in a radial structure, the transmission of electricity power from generation unit to terminal customs are competing for some of the major transmission branches. The commercial grid has to restrict the load in some of consumption buses to avoid overloading its transmission system when heavy volumes of the electricity power are transmitting from the centralized generation unit to remotely distributed customs [22] simultaneously, even if the grid has excessive generating capacities. This phenomenon becomes more obvious when renewable are incorporated in the generation, as the solar energy copeaks with smart building demands.

We provide the following example to illustrate the advantage of supplying smart building with local renewable generations. In Figure(1)a, a 20MW capacity generation unit is centrally located in bus 0. The consumptions are equally distributed in the remaining buses. All the buses are connected in a tree topology. We assume in this example that all the consumption buses has the same power load of 5MW. Therefore there is a 20MW power flow on the transmission line 1, while the power flow on transmission line 4 is 5MW. As the degree of loading caused thermal loss on the transmission line is proportional to the square of power that flow on the transmission line, the load on transmission line 1 is 15 times heavier than the load on transmission line 4 which will become the bottleneck for the whole transmission system.

However in Figure(1)b, a total capacity of 20MW generation unit is distributed in bus 0, 2, 4, 6 and 8. Bus 0, 2, 4, 6 and 8 has the corresponding generation capacity of 2.5MW, 5MW ,

5MW, 5MW and 2.5MW. The power load at the consumption buses are all 5MW which is the same as the previous condition. Under the conditions in our second example, the power flow in every transmission line is 2.5MW. All the transmission lines in this power system has the same load.

From the previous examples, we observe that the overloading of the main transmission branch will not become the bottleneck for renewable energy utilization when the renewable energies are mainly transmitting in its local branch. This motivate us to study the feasibility of integrating renewable generation and smart building in the same local MicroGrid and to further design a power management strategy to stabilize MicroGrid's operation condition thus utilizing the renewable energy in most efficient way. The MicroGrid we are studying has the following characteristics:

The power load in smart buildings and geo-distributed [23] renewable generation sites are connected to the MicroGrid. The power load for a single smart building is connected to one transformer. The renewable power generating units in one single location such as PV panel modules and wind turbine farms is also connected to one transformer. Each transformer is considered as one bus in the MicroGrid. Different buses in the microgrid are connected by the transmission lines. The energy generated by the renewable generating site is transmitting through the lines to smart building users. Contrary to the case of centralized generation, in which the electrical power flows in one way follows the direction from the generation bus as root to its sub-node, the actual direction of power flow is dynamic and determined by the realtime network operational condition. Finally, the MicroGrid requires or provides additional power from the grid. Microgrid connects to the grid through point of common coupling(PCC) through which the additional power can flow into the MicroGrid when renewable generation in MicroGrid is insufficient. Power generating buses have an inflexible and unpredictable power influx. Power consumption buses that are connected to the smart building has a controllable loads. Figure 1 draws an abstract picture of our renewable driven smart building power MicroGrid.

Realizing the concept of integration of distributed generation and smart buildings in an autonomy MicroGrid and further operating it properly are non-trivial tasks. Towards accomplishing these objectives, we need to address the following challenges:

•**Challenge 1: Protecting Power System Stability:** The reliable operation of electrical power system depends on keeping the power system parameter within the safe operation limits. These parameters such as power flows and bus voltages are determined by KCL,KVL and Ohm's laws

once power load on each bus is given. Failing to regulate the load on buses may seriously affect system's stability. Power system becomes even more volatile when distributed power generation is included.

•**Challenge 2:** *User satisfaction related load:* The thermal dynamics of the smart building relates to its air conditioning power consumptions. As users may feel uncomfortable when indoor temperature deviates the set point too much. Frequently regulating the smart building's air conditioning load may compromise user's satisfaction.

•**Challenge 3:** *System errors in data acquisition:* As converting these data from its original state to state in digital circuit in a high sampling frequency need complex structures such as A/D and amplifiers, introducing white Gaussian noise in the data collected from the sensors is inevitable. We should not sacrifice our accumulative performance too much under unreliable and random data.

To this end, we handle the previous stated difficulties by modeling the power management scheme in renewable driven smart building MicroGrid as convex optimization problem with a competitive stochastic solver. We will give an approximative power system model in section (IV), a user satisfaction model in section(V) and proposed a stochastic iterative algorithm in section (VI)

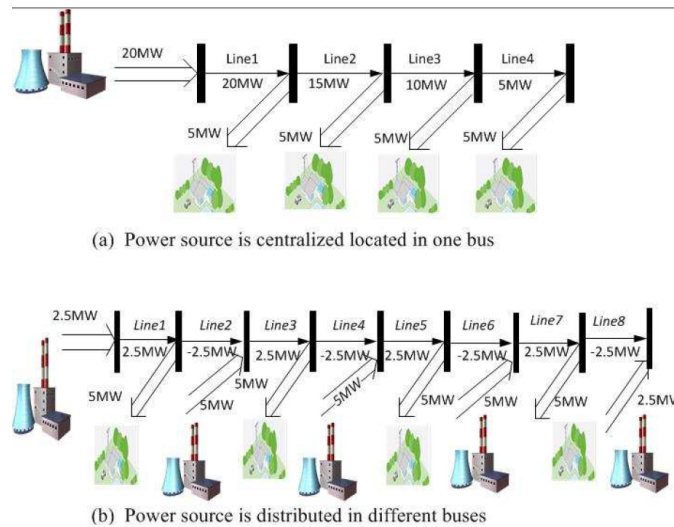


Fig. 1. Power load on the transmission line is different as a result of different power source placement.

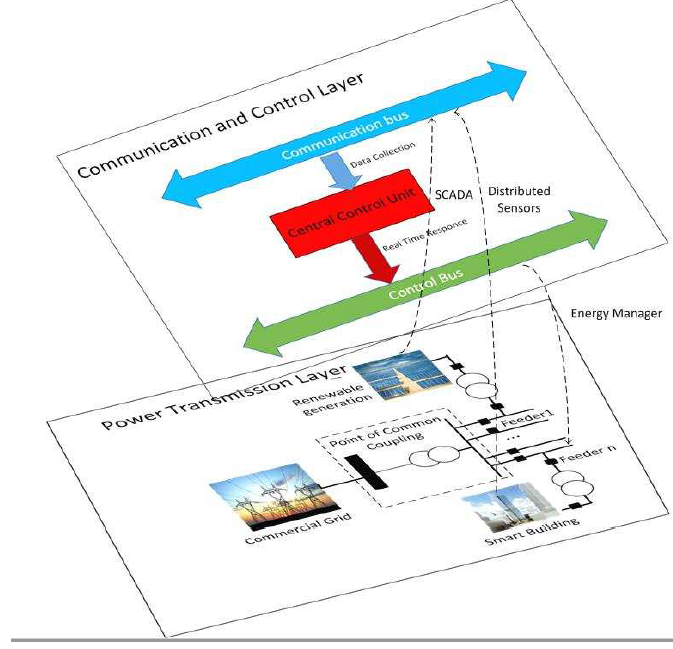


Fig. 2. System architecture of our renewable driven smart building power MicroGrid

IV. SYSTEM MODEL

A. General Power Grid Model

A general electricity power systems consists of generators, loads and power distribution systems. Generations and loads are connected by power distribution system. Power system is accessed through high voltage transformers that raise their voltage to power transmission level. In power grid models, these transformers are represented by buses (or feeders) as a generation of interface between power transmission system and end generations or loads. Figure 2 shows the basic structure and components of a transmission and distribution system. In describing transmission-line parameters, pi model is widely adopted to consider inductance in series and capacitance in parallel. Figure (3) illustrates the modeling of a transmission line.

Based on the previous background, the power network can be described in so termed network matrix model [24], [25]. Let $\mathcal{V} \triangleq \{0, 1, 2, \dots, N\}$ denotes the set of all buses, $\mathbf{u} \triangleq [u_0, u_1, \dots, u_N]^T$ refers to the vector of voltage at each buses, $\mathbf{i} \triangleq [i_0, i_1, \dots, i_N]^T$ refers to the vector of current at each buses. Each line is characterized by the admittance matrix $\mathbf{Y} = [Y_{n,m}]_{N \times N}$, which include line admittance $Y_{n,m} = G_{n,m} + iB_{n,m}$ and shunt admittance admittances $\bar{Y}_{n,m} = \bar{G}_{n,m} + i\bar{B}_{n,m}$ in the pi-model of line $n, m \in \xi$, and self-admittance $Y_{n,n} = -\sum_{m \neq n} (\bar{Y}_{n,m} + Y_{n,m})$. As the shunt

capacitance is so small relative to line impedance, we often neglect the shunt admittance part in network admittance matrix. \mathbf{u} and \mathbf{i} have the following relationship [26], [26]

$$\mathbf{i} = \mathbf{Y}\mathbf{u}. \quad (1)$$

This relationship is developed by applying KCL at each bus in the system to transform Olm's equation regarding the bus voltage and line current's to bus voltage and bus current injection relation.

The apparent power s_v on bus v has the following relation ship with its voltage and current injection.

$$s_v = u_v i_v^*, \quad (2)$$

where $s_v = p_v + iq_v$, p_v is the active power and q_v is the reactive power.

B. Linear Approximation for MicroGrid

We adopt the linear approximative model developed by S. Bolognani as the system model for our MiroGrid. This model is derived by taking the first order Tyler approximation form of the bus voltage as a function of bus power injection. The model is briefly described as follows:

We define matrix \mathbf{X} as

$$\begin{bmatrix} \mathbf{X} & \mathbf{1} \\ \mathbf{1}^T & 0 \end{bmatrix} = \begin{bmatrix} \mathbf{Y} & \mathbf{1} \\ \mathbf{1}^T & 0 \end{bmatrix}^{-1}, \quad (3)$$

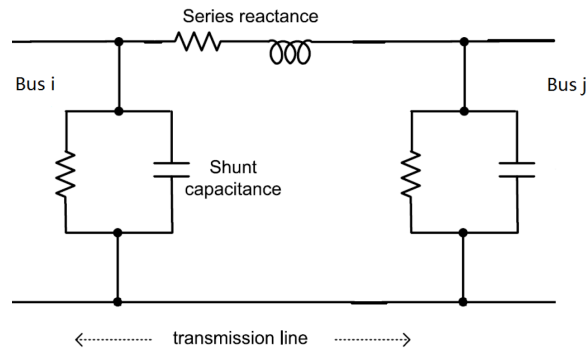


Fig. 3. Pi model of high voltage transmission line

where \mathbf{Y} is the admittance matrix defined in previous subsection.

The relationship between magnitude of voltage at the each bus \mathbf{u} and the power injection at each bus \mathbf{s} is given by

$$|u_v| \approx U_N + \frac{1}{U_N} [\Re([\mathbf{X}]_{i \neq 0} \mathbf{s})]_v, \quad (4)$$

and the total power loss on the transmission line are given by

$$p_l = \frac{1}{U_N^2} (\mathbf{p}^T \Re([\mathbf{X}]_{i \neq 0, j \neq 0}) \mathbf{p} + \mathbf{q}^T \Im([\mathbf{X}]_{i \neq 0, j \neq 0}) \mathbf{q}), \quad (5)$$

where $\mathbf{s} = \mathbf{p} + i\mathbf{q} \triangleq [s_1 \dots s_N]^T$

Consider our MicroGrid consists of $N + 1$ buses. These buses are numbered in set $\mathcal{V} = \{0, 1, 2, \dots, N\}$. The renewable generating is distributed among the buses $v \in \mathcal{V}_g$ with a time-varying passive power harvesting $p_g(v, t)$. Smart buildings is located on bus $v \in \mathcal{V}_c$ with adjustable power consumption $p_c(v, t)$. Our MicroGrid connects to grid through point of common coupling (PCC). Let the bus 0 be the PCC bus with fixed voltage $U_N e^{j\phi}$ as the requirement of current prevailing interface standard. Reactive power consumption is neutralized by the reactive compensation unit. For simplicity, we assume that the MicroGrid only consists of these two kinds of buses apart from bus 0. We also assume that bus $v \in \mathcal{V}_c$ only provide electrical energy for smart buildings.

Specifically in our model, The vector of power harvesting at power generation bus are denoted as:

$$\mathbf{p}_g(t) = [p_1(t), p_2(t), \dots, p_{N_g}(t)]^T, \quad \mathcal{V}_g = \{1, 2, \dots, N_g\}. \quad (6)$$

The vector of power consumption at consumption buses that are connected to the smart building are denoted as:

$$\begin{aligned} \mathbf{p}_c(t) &= [-p_{N_g+1}(t), -p_{N_g+2}(t), \dots, -p_N(t)]^T, \\ \mathcal{V}_c &= \{N_g + 1, N_g + 2, \dots, N\}. \end{aligned} \quad (7)$$

So that the power vector $\mathbf{p}_c(t), \mathbf{p}_g(t)$, at each bus can be written as the component of $\mathbf{s}_j(t)$

$$\mathbf{p}(t) = [\mathbf{p}_g(t), -\mathbf{p}_c(t)]^T. \quad (8)$$

As reactive power is required to compensate at each buses by current MicroGrid standard, we only consider the active power at each buses.

$$\mathbf{s}(t) = \mathbf{p}(t). \quad (9)$$

The matrix \mathbf{X} can be composed to the sub-matrix that corresponds to the dimension of N_g and N_c

$$\Re(\mathbf{X}) = \begin{bmatrix} 0 & 0 & 0 \\ 0 & \mathbf{M} & \mathbf{N} \\ 0 & \mathbf{N}^T & \mathbf{Q} \end{bmatrix}, \quad (10)$$

with $\mathbf{M} \in \mathbb{R}^{N_g \times N_g}$, $\mathbf{N} \in \mathbb{R}^{N_g \times N_c}$ and $\mathbf{Q} \in \mathbb{R}^{N_c \times N_c}$. By substituting the decomposition of matrix \mathbf{X} (11) and power consumption vector $\mathbf{p}(t)$ (9) into power loss equation (5), we have

$$\begin{aligned} p_l(t) &= [\mathbf{p}_g(t)^T, -\mathbf{p}_c(t)^T] \begin{bmatrix} \mathbf{M} & \mathbf{N} \\ \mathbf{N}^T & \mathbf{Q} \end{bmatrix} [\mathbf{p}_g(t)^T, -\mathbf{p}_c(t)^T]^T \\ &= \frac{1}{U_N^2} (\mathbf{p}_g(t)^T \mathbf{M} \mathbf{p}_g(t) - 2\mathbf{p}_g(t)^T \mathbf{N} \mathbf{p}_c(t) + \mathbf{p}_c(t)^T \mathbf{Q} \mathbf{p}_c(t)). \end{aligned} \quad (11)$$

Similarly by substituting the decomposition of matrix \mathbf{X} (11) and power consumption vector $\mathbf{p}(t)$ (9) into bus voltage magnitude equation (4), we have

$$\begin{aligned} |\mathbf{u}| &= U_N + \frac{1}{U_N} \begin{bmatrix} \mathbf{M} & \mathbf{N} \\ \mathbf{N}^T & \mathbf{Q} \end{bmatrix} [\mathbf{p}_g^T, -\mathbf{p}_c^T]^T \\ &= U_N + \frac{1}{U_N} [(\mathbf{M} \mathbf{p}_g(t) - \mathbf{N} \mathbf{p}_c(t))^T, (\mathbf{N}^T \mathbf{p}_g(t) - \mathbf{Q} \mathbf{p}_c(t))^T]^T. \end{aligned} \quad (12)$$

V. PROBLEM FORMULATION

In this section, we first introduce our framework of optimal power management in renewable driven smart building MicroGrid with renewable generation in a systematic scale. We then develop our user satisfaction and electricity consumption balanced (USECB) profit model with the constrain region of power network in a concrete notation of a function of power injection at each bus. Based on our USECB model, objective profit is quantified as a measurement of the overall achievement which is user satisfactory related. Our power management strategy is based on maximizing the net profit in our USECB model as an objective function subject to the constraint of power capacity and power network safe operation limit. Finally, we model the practical problem in noise contaminated environment as a stochastic optimization problem aiming at minimizing the expectation of a stochastic function.

A. Smart Building Power Management Overview

As the majority of devices integrated in the MicroGrid are power electronic based, MicroGrid is smartened by electronic systems' smooth and accurate control ability and fast computation power. Thanks to the state-of-arts power electronic system, system cores namely supervisory control and data acquisition system (SCADA) and user end devices such as distributed sensors that are monitoring the dynamic status of the user's systems and power management modules that are smartly controlling and adjusting user's loads are highly integrated in the controlling system to give MicroGrid a high degree of flexibility to act as a single controlled unity. This makes it possible for us to apply a centralized management strategy rather than a distributed one as the low complexity of the small MicroGrid system, high robustness of the control system and the little transmission delay in the whole system. A centralized control unit exhibits as the core for gathering information about the overall system's status and generating control signals based on the assembled optimization programs.

At the beginning of each time slot, information from distributed sensors are gathered at the central control unit. The information gathered at the central control unit are real time inside temperature of each building at bus v $c_{in}(v, t)$, outside temperature of each building at bus v $c_{out}(v, t)$, power injection $p_g(v, t)$ at each generating bus $v \in \mathcal{V}_g$. The centralized control unit make real time response by adjusting the load on consumption buses. This decision is based on maximizing an objective function of our USECB model without harming the system stability by fluctuating bus voltage too much. The controlling strategy utilize in time censoring data while the previous result is also considered.

B. Quantifying Objective Profit

We put forward the concept of net profit in our USECB model that achieves the compromising between power reliance on outside grid and user's satisfaction maximizing. To incorporate the concept of our objective profit in USECB model in the framework of real-time power management, the net profits in our USECB model are evaluated on a per time slot bases.

Definition 1 *Given the air conditioning related flexible power consumption at each bus $\mathbf{p}_c(t)$ (the concept of air conditioning related flexible power consumption will be explained as follows),*

the USECB net profit $\pi(\mathbf{p}_c(t))$ is defined as user's overall satisfaction related revenue minus its power cost from outside commercial grid.

We explore the modeling and computation of USECB in the following part. We first develop the concept of AC related flexible power consumption. Though the total power consumption can be of multiple types such as AC systems, venting, lighting and absolute user demand. In this paper, we only consider adjusting the load that supplies AC systems and study the effect of managing these kinds load supplied to AC systems as other types of power consumption have limited degree of flexibility or its impact on the overall system is negligible.

Given the power consumption $p_c(v, t)$ at time t for the smart building that are connected to bus v , we denote the satisfactory revenue of its users as $U(p_c(v, t), t)$ by cooling the indoor temperature closer to user's set level. We also denote λ as the unit electricity price for power taken from outside commercial grid. Therefore the net profit in USECB model can be expressed in the following form:

$$\pi(\mathbf{p}_c(t), t) = \sum_{v \in \mathcal{V}_g} U(p_c(v, t), t) - \lambda p_0(t). \quad (13)$$

User Satisfaction Related Revenue In many research papers such as [27], [28], the utility function of AC devices is usually set to be proportional to the square of difference between the actual inside temperature and set temperature.

$$U(p_c(v, t), t) = -\beta(c_{in}(v, t+1) - c_{set}(v))^2. \quad (14)$$

where $c_{set}(v)$ is the objective goal set by user in bus v . User in bus v wish the temperature to be adjusted around the set temperature $c_{set}(v)$ at which the user will feel most satisfied. $c_{in}(v, t+1)$ is the predictive inside temperature in the next time slot which is sum up by the current inside temperature and heating coming from the outside and the cooling power refrigerated by AC. According to the thermodynamic equation, we have

$$(c_{in}(p_c(v, t), t+1) - c_{in}(v, t))C_{room} = \lambda_{room}(c_{out}(v, t) - c_{in}(v, t))\Delta t + \eta', p_c(v, t)\Delta t. \quad (15)$$

where C_{room} is specific heat capacity of the smart building, λ_{room} is the heat transfer coefficient between smart building and outside, η' is the cooling efficiency of the AC. By taking (15) into

(14), we have the following relationship between the realtime AC injection power and users satisfaction.

$$U(p_c(v, t), t) = -\beta(c_{in}(v, t) + \frac{\lambda_{room}}{C_{room}}(c_{out}(v, t) - c_{in}(v, t))\Delta t + \frac{\eta'}{C_{room}}p_c(v, t)\Delta t - c_{set}(v))^2. \quad (16)$$

To simplify the model by eliminating the redundant variables, we set $\frac{\lambda_{room}}{C_{room}} = \alpha_1$, $\frac{\eta' p_c(v, t)}{C_{room}} = \alpha_2$, equation (16) is written as follows:

$$U(p_c(v, t), t) = -\beta(c_{in}(v, t) + \alpha_1(c_{in}(v, t) - c_{out}(v, t))\Delta t + \alpha_2 p_c(v, t)\Delta t - c_{set}(v))^2. \quad (17)$$

The overall net revenue of all users written as the summation of user welfare in all buses in vector form $\mathbf{p}_c(t)$ can be denoted as:

$$\begin{aligned} U(\mathbf{p}_c(t), t) &= \sum_{v \in \mathcal{V}_c} U(p_c(v, t), t) \\ &= -\beta(\mathbf{c}_{in}(t) + \Lambda_1(\mathbf{c}_{out}(t) - \mathbf{c}_{in}(t))\Delta t \\ &\quad - \Lambda_2 \mathbf{p}_c(t)\Delta t - \mathbf{c}_{set}(v))^T (\mathbf{c}_{in}(t) + \Lambda_1(\mathbf{c}_{out}(t) - \mathbf{c}_{in}(t))\Delta t \\ &\quad - \Lambda_2 \mathbf{p}_c(t)\Delta t - \mathbf{c}_{set}(t)), \end{aligned} \quad (18)$$

where $\Lambda_1 = \text{diag}(\alpha_1)$ and $\Lambda_2 = \text{diag}(\alpha_2)$

Power Cost to Grid Apart from fixed cost for MicroGrid's basic maintenance, the major additional cost for MicroGrid is the cost to procure additional power from outside commercial grid. We assume the electricity cost is proportional to the power intake from the grid $p_0(t)$ at unit price of λ . Here we denote $p_0(t)$ as a function of $p_c(v, t)$ by the law of energy conservation and power loss equation

$$\begin{aligned} p_0(t) &= \mathbf{1}^T \mathbf{p}_c(t) - \mathbf{1}^T \mathbf{p}_g(t) \\ &\quad + \frac{1}{U_N^2} (\mathbf{p}_g(t)^T \mathbf{M} \mathbf{p}_g(t) - 2\mathbf{p}_g(t)^T \mathbf{N} \mathbf{p}_c(t) + \mathbf{p}_c(t)^T \mathbf{Q} \mathbf{p}_c(t)). \end{aligned} \quad (19)$$

C. Load Constraint in MicroGrid

To maintain MicroGrid system stability, the magnitude of voltage should be kept within safe operation limit.

$$v_{min} \leq |\mathbf{u}| \leq v_{max}. \quad (20)$$

The power consumption at each bus should be remained within its capacity.

$$p_{min} \leq \mathbf{p}_c(t) \leq p_{max}. \quad (21)$$

We denote set \mathcal{A} as the convex set of power constraint which satisfies the voltage stable condition and maximum power constrain.

$$\begin{aligned} \mathbf{p}_c(t) \in \mathcal{A} : \{ \mathbf{p}_c(t) \mid v_{min} \leq |\mathbf{u}(U_N, \mathbf{p}_c(t))| \leq v_{max} \\ \cap p_{min} \leq \mathbf{p}_c(t) \leq p_{max} \}. \end{aligned} \quad (22)$$

D. Power Management Problem in Noise Environment

As $\pi(\mathbf{p}_c(t), t)$ can be written as:

$$\pi(\mathbf{p}_c(t), t) = \lambda f(\mathbf{p}_c(t), t) + c, \quad (23)$$

where

$$\begin{aligned} f(\mathbf{p}_c(t), t) = & \frac{\beta}{\lambda} [(\mathbf{p}_c(t)^T \Lambda_1 \Lambda_2 \mathbf{p}_c(t) \Delta t^2 \\ & - 2(\mathbf{c}_{in}(t) + \Lambda_1(\mathbf{c}_{out}(t) - \mathbf{c}_{in}(t))\Delta t - \mathbf{c}_{set}(t))^T \Lambda_2 \mathbf{p}_c(t) \Delta t] \\ & + \mathbf{1}^T \mathbf{p}_c(t) + \lambda \frac{1}{U_N^2} (-2\mathbf{p}_g^T \mathbf{N} \mathbf{p}_c + \mathbf{p}_c^T \mathbf{Q} \mathbf{p}_c) \\ c = & (\mathbf{c}_{in}(t) + \Lambda_1(\mathbf{c}_{out}(t) - \mathbf{c}_{in}(t)))^T (\mathbf{c}_{in}(t) + \Lambda_1(\mathbf{c}_{out}(t) - \mathbf{c}_{in}(t)) + \mathbf{1}^T \mathbf{p}_g. \end{aligned} \quad (24)$$

Maximizing $\pi(\mathbf{p}_c(t), t)$ is equally as minimizing $f(\mathbf{p}_c(t), t)$. As the data obtained from the distributed sensors are always the noise corrupted version of the their actual value, we consider our the optimal smart building power management problem in noise contaminated environment as a stochastic optimization problem in statistical point of view. We observe function $f(\mathbf{p}_c(t); \hat{Z})$ in multiple perspective. $f(\mathbf{p}_c(t); \hat{Z})$ is notated as a clear deterministic analytical form as a function of $\mathbf{p}_c(t)$ and Z , where Z is the parameter of f namely \mathbf{c}_{in} , \mathbf{c}_{out} and \mathbf{p}_g . However these parameters in Z appears in the form of random variables $\hat{Z} \sim P$ when noise is introduced. In this way, $f(\mathbf{p}_c(t); \hat{Z})$ will be a random variable of which distribution is a function of $\mathbf{p}_c(t)$. $f(\mathbf{p}_c(t); \hat{Z})$ is no longer a deterministic function of $\mathbf{p}_c(t)$. Instead random variables $f(\mathbf{p}_c(t); \hat{Z})$ only follows the distribution that is determined as a function of $\mathbf{p}_c(t)$. However its statistical properties such as expectation is still a deterministic function of $\mathbf{p}_c(t)$. Under the previous context, we model

the problem of optimal smart building power management as minimizing the expectation of a randomized function rather than its exact value.

$$\begin{aligned} \min : & \mathbb{E}[f(; \hat{Z})] \\ \text{s.t.} : & \mathbf{p}_c(t) \in \mathcal{A}. \end{aligned} \tag{25}$$

VI. ALGORITHM DESIGN AND CONVERGENCE ANALYSIS

As noise corrupted environment impedes us from deriving any exact analytical form of the expectation function, this rules out us to find any analytical solution or applying approximative approaches in convex optimization directly. Therefore theoretical upper bound is not achievable when the measurement is corrupted by noise. Indeed we exploit Bregmen projection based mirror decent algorithm to iterate the objective variable $\mathbf{p}_c(t)$ that gradually converges to the optimization point of the expectation functions. In this section, we first introduce our Bregmen projection based mirror decent algorithm and applies our algorithm to the specific problem of optimal power management in smart building in noise corrupted environment. Convergence analysis is provided in the final part of this section as a theoretical base. The notations and discussions in convergence analysis part are made intentionally independent of other parts of the paper in order to present the proof in a mathematically general way [29], [30].

A. Stochastic Approximation Solver

We begin introducing our Bregmen projection based mirror decent algorithm by first presenting the definition of Bregmen function and divergence. The Bregmen divergence associated with ψ is defined as:

Definition 2 *Let ψ denotes a continuous differentiable function. The Bregmen divergence associated with ψ is defined as:*

$$B_\psi(\boldsymbol{\omega}, \mathbf{v}) = \psi(\boldsymbol{\omega}) - \psi(\mathbf{v}) - \langle \nabla \psi(\mathbf{v}), \boldsymbol{\omega} - \mathbf{v} \rangle. \tag{26}$$

Our online mirror decent method is described as the follows:

Step 1: Online Mirror Decent

$$\omega_{p_c^0}(t+1) = \nabla \psi^d(\nabla \psi(\mathbf{p}_c(t)) - \eta \nabla f(\mathbf{p}_c(t))), \tag{27}$$

where ψ^d denotes the dual function of ψ .

Specifically, we use square of Eculid norm $\psi(\omega) = \frac{1}{2}\|\omega\|_2^2$ in our specific problem. The mirror decent step can written as follows in analytical form [31]:

$$\begin{aligned} \omega_{p_c^0}(t+1) = & \mathbf{p}_c(t) - \eta(\Lambda_2\beta\Delta t(\mathbf{c}_{in}(t+1) + \Lambda_1(\mathbf{c}_{in}(t+1) - \mathbf{c}_{out}(t+1))\Delta t \\ & - \Lambda_2\mathbf{p}_c(t+1)\Delta t - \mathbf{c}_{set}(t+1)) + \lambda\mathbf{1} + \lambda\frac{1}{U_N^2}(-2\mathbf{N}\mathbf{p}_g(t+1) + 2\mathbf{Q}\mathbf{p}_c(t)). \end{aligned} \quad (28)$$

Step 2: Bregmen Projection

$$\mathbf{p}_c(t+1) = \arg \min_{x \in \mathcal{A}} B_\psi(x, \omega_{p_c^0}(t+1)). \quad (29)$$

Comparing with the theoretical optimal solution $\mathbf{p}_c^*(t)$ at time slot t , the iterative result $\mathbf{p}_c(t)$ obtained by our algorithm has a utility loss of $\mathbb{E}(f(\mathbf{p}_c(t))) - \mathbb{E}(f(\mathbf{p}_c^*(t)))$. Under the assumption that the distribution of f stays the same over time T , the accumulative utility loss over time T $R_n = \sum_{t=1}^T f(\mathbf{a}_t) - \inf \sum_{t=1}^T f(\mathbf{a}^*)$ can be upper bounded by a function of $O(\sqrt{T})$ which will be proved in the later part of this section at convergence analysis.

B. Convergence Analysis

We recall that accumulative regret rate is defined as:

$$R_n = \sum_{t=1}^T f(\mathbf{a}_t) - \inf \sum_{t=1}^T f(\mathbf{a}^*). \quad (30)$$

We prove the convergence of the algorithm by giving an upper-bound of R_n . Before going to the formal proof, we first introduce the three lemmas that our proof relies on.

Lemma 1 *Let $\mathcal{A} \in \overline{\mathcal{D}}$ be a closed and convex set such that $\mathcal{A} \cap \mathcal{D} \neq \emptyset$. Then, $\forall x \in \mathcal{D}$,*

$$b = \arg \min_{a \in \mathcal{A}} B_\psi(a, x), \quad (31)$$

exists and is unique. Moreover $b \in \mathcal{A} \cap \mathcal{D}$, and $\forall a \in \mathcal{A}$,

$$B_\psi(a, x) \geq B_\psi(a, b) + B_\psi(b, x). \quad (32)$$

Lemma 2

$$B_\psi(x, y) + B_\psi(y, z) = B_\psi(x, z) + \langle x - y, \psi'(z) - \psi'(y) \rangle. \quad (33)$$

Lemma 3

$$B_\psi(x, y) - B_\psi(z, y) = \psi(x) - \psi(z) + \langle x - z, \psi'(x) - \psi'(z) \rangle. \quad (34)$$

Theorem 1 Assuming that ψ is α convex. The dual norm of subgradient satisfies $\|f'(\omega)\|_* \leq G_*$ for any ω . And the iterative point \mathbf{a}_t is set as close to the optimization point as for any $B_\psi(\mathbf{a}_*, \mathbf{a}_t) < D^2$. And the iteration step is set as $\eta_t = \frac{D\sqrt{\alpha}}{G_*\sqrt{t}}$. Then we have the following convergence bound.

$$P(R_n \geq \frac{2DG_*\sqrt{T}}{\sqrt{\alpha}} + \varepsilon) \leq \exp(-\frac{\alpha\varepsilon^2}{16TD^2G_*^2}). \quad (35)$$

Proof 1 By the definition of subgradient, we have

$$\begin{aligned} f(\mathbf{a}_t) - f(\mathbf{a}^*) \\ \leq \langle \mathbf{a}_t - \mathbf{a}^*, f'_t(\mathbf{a}_t) \rangle + \langle \mathbf{a}_t - \mathbf{a}^*, f'(\mathbf{a}_t) - f'_t(\mathbf{a}_t) \rangle. \end{aligned} \quad (36)$$

Using the iteration equation (27), we have

$$\begin{aligned} \langle \mathbf{a}_t - \mathbf{a}^*, f'_t(\mathbf{a}_t) \rangle \\ = \frac{1}{\eta_t} \langle \mathbf{a} - \mathbf{a}_t, \psi'(\mathbf{w}_{t+1}) - \psi'(\mathbf{a}_t) \rangle. \end{aligned} \quad (37)$$

Applying Lemma 1 and Lemma 2, we have

$$\begin{aligned} & \frac{1}{\eta_t} \langle \mathbf{a} - \mathbf{a}_t, \psi'(\mathbf{w}_{t+1}) - \psi'(\mathbf{a}_t) \rangle \\ &= \frac{1}{\eta_t} \langle a - a_t, \psi'(w_{t+1}) - \psi'(a_t) \rangle \\ &= \frac{1}{\eta_t} (B_\psi(a, a_t) + B_\psi(a_t, w_{t+1}) - B_\psi(a, w_{t+1})) \\ &\leq \frac{1}{\eta_t} (B_\psi(a, a_t) + B_\psi(a_t, w_{t+1}) - B_\psi(a, a_{t+1}) - B_\psi(a_{t+1}, w_{t+1})). \end{aligned} \quad (38)$$

To sum up, we have

$$\begin{aligned} & \sum_{t=1}^T \langle \mathbf{a}_t - \mathbf{a}^*, f'_t(\mathbf{a}_t) \rangle \\ &\leq \sum_{t=1}^T \frac{1}{\eta_t} (B_\psi(a, a_t) + B_\psi(a_t, w_{t+1}) - B_\psi(a, a_{t+1}) - B_\psi(a_{t+1}, w_{t+1})) \\ &= \frac{1}{\eta_1} B_\psi(a, a_1) + \sum_{t=2}^T \left(\frac{1}{\eta_t} - \frac{1}{\eta_{t-1}} \right) B_\psi(a, a_t) + \sum_{t=1}^T \frac{1}{\eta_t} (B_\psi(a_t, w_{t+1}) - B_\psi(a_{t+1}, w_{t+1})). \end{aligned} \quad (39)$$

Applying Lemma 3, we have

$$\begin{aligned} & B_\psi(a_t, w_{t+1}) - B_\psi(a_{t+1}, w_{t+1}) \\ &= \psi(a_t) - \psi(a_{t+1}) + \langle \mathbf{a}_{t+1} - \mathbf{a}_t, \psi'(\mathbf{w}_{t+1}) \rangle. \end{aligned} \quad (40)$$

Applying the α convex property of Bregmen Divergence

$$\begin{aligned}
& \psi(a_t) - \psi(a_{t+1}) + \langle \mathbf{a}_{t+1} - \mathbf{a}_t, \psi'(\mathbf{w}_{t+1}) \rangle \\
& \leq \langle \mathbf{a}_t - \mathbf{a}_{t+1}, \psi'(\mathbf{w}_t) \rangle - \frac{\alpha}{2} \|a_t - a_{t+1}\|^2 + \langle \mathbf{a}_t - \mathbf{a}_{t+1}, \psi'(\mathbf{w}_{t+1}) \rangle \\
& = -\eta_t \langle f'(a_t), a_t - a_{t+1} \rangle - \frac{\alpha}{2} \|a_t - a_{t+1}\|^2 \\
& \leq \eta_t G_* \|a_t - a_{t+1}\| - \frac{\alpha}{2} \|a_t - a_{t+1}\|^2 \\
& \leq \frac{(\eta_t G_*)^2}{2\alpha}.
\end{aligned} \tag{41}$$

Let \mathcal{F}_t be a filtration of with $Z_\tau \in \mathcal{F}_t$ for $\tau \leq t$. Since $\mathbf{w}_t \in \mathcal{F}_{t-1}$

$$\mathbb{E}[\langle \mathbf{a}_t - \mathbf{a}^*, f'(\mathbf{a}_t) - f'_t(\mathbf{a}_t) \rangle | \mathcal{F}_{t-1}] = \langle \mathbf{a}_t - \mathbf{a}^*, f'(\mathbf{a}_t) - \mathbb{E}[f'_t(\mathbf{a}_t) | \mathcal{F}_{t-1}] \rangle = 0. \tag{42}$$

Thus $\sum_{t=1}^T \langle \mathbf{a}_t - \mathbf{a}^*, f'(\mathbf{a}_t) - f'_t(\mathbf{a}_t) \rangle$ is a martingale difference sequence

$$\langle \mathbf{a}_t - \mathbf{a}^*, f'(\mathbf{a}_t) - f'_t(\mathbf{a}_t) \rangle \leq \|\mathbf{a}_t - \mathbf{a}^*\| \|f'(\mathbf{a}_t) - f'_t(\mathbf{a}_t)\|_* \leq 2\sqrt{2/\alpha} DG_*. \tag{43}$$

Defining $\sum_{t=1}^T \langle \mathbf{a}_t - \mathbf{a}^*, f'(\mathbf{a}_t) - f'_t(\mathbf{a}_t) \rangle = \gamma_T$.

Applying Azuma's inequality, we have

$$P(\gamma_T \geq \epsilon) \leq \exp\left(-\frac{\alpha \epsilon^2}{16TD^2G_*^2}\right). \tag{44}$$

So that applying the previous derived inequality, finally we have

$$\begin{aligned}
R_n & \leq \sum_{t=1}^T (\langle \mathbf{a}_t - \mathbf{a}^*, f'_t(\mathbf{a}_t) \rangle + \langle \mathbf{a}_t - \mathbf{a}^*, f'(\mathbf{a}_t) - f'_t(\mathbf{a}_t) \rangle) \\
& \leq \frac{1}{\eta_1} B_\psi(a, a_1) + \sum_{t=2}^T \left(\frac{1}{\eta_t} - \frac{1}{\eta_{t-1}}\right) B_\psi(a, a_t) \\
& \quad + \sum_{t=1}^T \frac{1}{\eta_t} (B_\psi(a_t, w_{t+1}) - B_\psi(a_{t+1}, w_{t+1})) + \langle \mathbf{a}_t - \mathbf{a}^*, f'(\mathbf{a}_t) - f'_t(\mathbf{a}_t) \rangle \\
& \leq \frac{D^2}{\eta_T} + \frac{G_*^2}{2\alpha} \sum_{t=1}^T \eta_t + \gamma_T \\
& < \frac{DG_*\sqrt{T}}{\sqrt{\alpha}} + \sum_{t=1}^T \frac{DG_*}{\sqrt{\alpha}} (\sqrt{t} - \sqrt{t-1}) + \gamma_T \\
& = \frac{2DG_*\sqrt{T}}{\sqrt{\alpha}} + \gamma_T.
\end{aligned} \tag{45}$$

Applying inequality (44), we finally get,

$$P(R_n \geq 2\frac{DG_*\sqrt{T}}{\sqrt{\alpha}} + \epsilon) \leq \exp\left(-\frac{\alpha \epsilon^2}{16TD^2G_*^2}\right). \tag{46}$$

VII. SIMULATION

We test our novel stochastic power management approach on IEEE 37 buses which depicts the real power distribution network model from Southern California Edison. The topology of IEEE 37 buses is shown in Fig.(4). The ideal optimized power injection scheme is determined by solving the deterministic convex optimization problem (25) directly based on the exact data which provides a theoretical lower bound for the objective function (25). Performance is tested both by the result of actual power loss on the transmission line and power intake from outside grid. Two experiments are conducted in our whole simulation process.

The dataset includes solar generation data gathered at three independent solar generation unit installed for the same home. In the dataset, the sensors monitors the amount of real time power generation at each unit in August 12th 2011 from 6am to 6pm which covers the full daytime generation range for PV. The normalized generation data is shown in Fig.(6). Our intension to choose the generation dataset from Smart Project [32], [33] are based on the following aspects. The dataset contains general patterns for PV unit daytime generation variation in a typical sunny day. Variations caused by sun rise and fall and fluctuations caused by clouds are obvious in this dataset. The dataset also includes different samples which reflects the variation in solar power harvesting at different sites that have the approximately same sunlight conditions.

In our simulation, we assume that three PV generation sites of 12MW are placed respectively on bus 725, 731 and 741. The normalized generation data from these three solar generation units in Smart project are utilized in our simulation to represent real-time PV generation variation

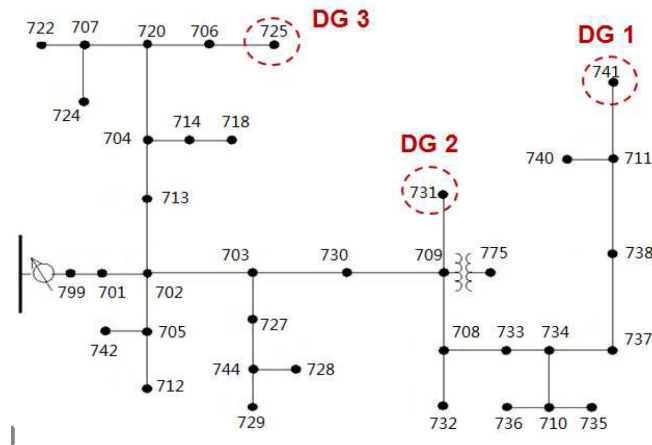


Fig. 4. The structure of IEEE 37 buses used in our simulation where distributed generations are on bus 725, 731 and 741.

on a per 48 sec bases. The root bus 799 is set as the PCC that is connected to the grid. The remaining buses are set as the consumption buses of which the power requirement includes an inflexible 0.6MW loads plus an adjustable loads that are mainly driven by smart building cooling needs. The maximum rate of central AC is set as 1.2MW at each buses under which it can cool down the building at degrees per T_g per minute. We neglect the power consumption of central AC when it works in standby condition. T_g is set differently following the distribution of $N(1=p_{max}; 0:16=p_{max})$ at each consumption buses. Other thermostats parameters regarding the smart buildings are obtained from real time indoor and outdoor temperature data obtain from one smart home in Smart project [18]. Renewable generation data is observed with a white Gaussian Noise 30data is observed with a white Gaussian noise of variance 3.

In our first group of experiment, we are testing the convergence property of our algorithm in ideal steady cases. The static data is used in this experiment. Indoor temperature is set fixed following the distribution of $N(65; 5)$ in smart buildings connected to each bus. Outdoor temperature and renewable generation are set fixed at the data from Smart project [18] at 7am. Stochastic scheme and exact scheme are both tested in this simulation. Figure(7) shows the performance of stochastic and exact method measured by the value of objective minimization function. The red line is the exact scheme comparing with our stochastic one in blue. The result of our stochastic scheme converges in a few iteration steps with a much better performance than the exact one which highly fluctuates above our stochastic performance curve.

In our second group of experiment, we are testing our algorithm in actual dynamic environment. The data collected at each time slot is their real time actual value plus a white Gaussian noise as described in previous context. Figure (8) shows variation of air-conditioning power consumption at bus 701, where the blue line indicates our algorithm and the red line indicates the exact scheme. Our algorithm has a much smoother curve while the exact scheme adopts the noisy pattern of the observed data. Figure (9) shows the actual temperature variation of the smart building connected at bus 701. Temperature is conditioned around the set goal in spite of the presence of noise. Figure (10) shows the actual power loss on the transmission line. The total power loss is reduced in the period of high renewable penetration as the increased dependency on local renewable which follows our assumption that effective local power usage reduces the load on the transmission line. Figure (11) shows the actual power intake from the grid. As the high renewable generation occurs simultaneously with high smart building power demand, local renewables are nearly sufficient to supply smart building in peak hour. By incorporating

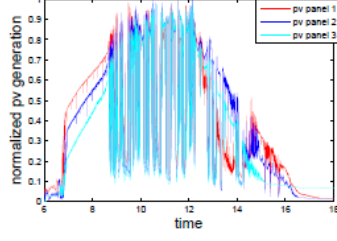


Fig. 6. Renewable generation data from 6am to 6pm

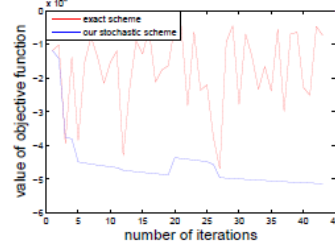


Fig. 7. Value of objective function in static case

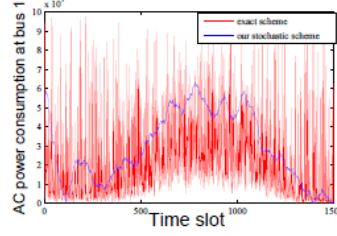


Fig. 8. AC power consumption at bus 1 stochastic scheme vs exact one

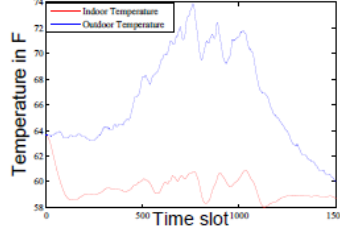


Fig. 9. Inside and outside temperature

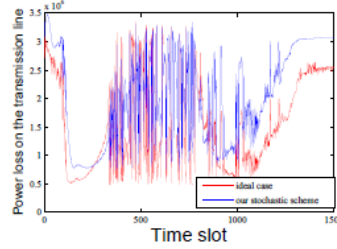


Fig. 10. Power loss stochastic result vs ideal case

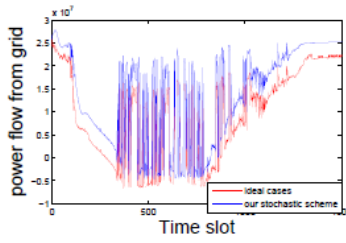


Fig. 11. Power intake from grid stochastic result vs ideal case

local renewables in MicroGrid, not only grid capacity required for smart building is reduced but also the consumption pattern is inversed that smart building take less powers in traditional peak demand period. Our algorithm can approach the performance of the ideal schemes in most of time in both of these two metrics. Overall the experiment has tested the feasibility of our motivation of supplying the smart building with local renewable, the effectiveness of our USECB mode together with the effectiveness of our algorithm to filter the noise, converge to the trend of actual data dynamics and close to the performance in ideal case.

VIII. CONCLUSIONS

In this paper, we have outlooked the prospect of utilizing the local MicroGrid to drive the smart building and further investigated a optimal power management strategy. A USECB model has been presented to achieve balance between user welfare and external power consumption.

Based the basis of proposed model, a Bregemen projection based mirror decent algorithm has been developed to optimize objective function in noise contaminated environment. Our algorithm has achieved an accumulative $O(\sqrt{T})$ loss than theoretical bound in steady state.

We have tested the performance our algorithm in our simulation. We have proposed three metrics in our simulation which are power losses, external power consumption and objective function values. In the period of high local renewable penetration, power losses and external power consumption have been both reduced. Our algorithm have a smooth power management curve while approaching the performance of idea cases in temperature control and all these three metrics, comparing with the exact scheme that are highly unstable.

Actually our algorithm can be extended to a broad variety of power grid control tasks in the presence of renewable generations which are characterized by frequent fluctuations and high degree of uncertainties. Motivated by the recent trend of installing mass distributed power storage devices to cope with the variation in distributed generation, we intend to incorporate the part of power management in microgrid with distributed storage in our future work.

REFERENCES

- [1] Q. Wang, X. Liu, J. Du, and F. Kong, "Smart charging for electric vehicles: A survey from the algorithmic perspective," *IEEE Communications Surveys & Tutorials*, vol. 18, no. 2, pp. 1500–1517, 2016.
- [2] K. Cai, X. Li, J. Du, Y.-C. Wu, and F. Gao, "Cfo estimation in ofdm systems under timing and channel length uncertainties with model averaging," *IEEE Transactions on Wireless Communications*, vol. 9, no. 3, pp. 970–974, 2010.
- [3] J. E. Braun, "Load control using building thermal mass," *Journal of solar energy engineering*, vol. 125, no. 3, pp. 292–301, 2003.
- [4] J. M. Sinopoli, *Smart buildings systems for architects, owners and builders*. Butterworth-Heinemann, 2009.
- [5] N. Council, "Technical analysis of the august 14, 2003, blackout: what happened, why and what did we learn?" *NERC, Princeton, NJ, Tech. Rep.*, 2004.
- [6] S. Bolognani and S. Zampieri, "A distributed control strategy for reactive power compensation in smart microgrids," *IEEE Transactions on Automatic Control*, vol. 58, no. 11, pp. 2818–2833, 2013.
- [7] J. Du, X. Liu, and L. Rao, "Proactive doppler shift compensation in vehicular cyber-physical systems," *IEEE/ACM Transactions on Networking*, 2018.
- [8] D. Schrank, B. Eisele, and T. Lomax, "The 2012 urban mobility report." in *Texas Transportation Institute*, 2012.
- [9] Y. Gu, "Greening Geographical Power Allocation for Cellular Networks," *arXiv preprint arXiv:1802.*, 2018.
- [10] P. Xu, P. Haves, M. A. Piette, and L. Zagreus, "Demand shifting with thermal mass in large commercial buildings: Field tests, simulation and audits," 2005.
- [11] B. Ramanathan and V. Vittal, "A framework for evaluation of advanced direct load control with minimum disruption," *IEEE Transactions on Power Systems*, vol. 23, no. 4, pp. 1681–1688, 2008.
- [12] G. P. Henze, C. Felsmann, and G. Knabe, "Evaluation of optimal control for active and passive building thermal storage," *International Journal of Thermal Sciences*, vol. 43, no. 2, pp. 173–183, 2004.

- [13] M. Farivar and S. H. Low, “Branch flow model: Relaxations and convexification part i,” *IEEE Transactions on Power Systems*, vol. 28, no. 3, pp. 2554–2564, 2013.
- [14] Q. Wang, “Energy Spatio-Temporal Pattern Prediction for Electric Vehicle Networks,” *arXiv preprint arXiv:1802.04931*, 2018.
- [15] —, “Branch flow model: Relaxations and convexification,” in *Decision and Control (CDC), 2012 IEEE 51st Annual Conference on*. IEEE, 2012, pp. 3672–3679.
- [16] S. Suryanarayanan and J. Mitra, “Enabling technologies for the customer-driven microgrid,” in *Power & Energy Society General Meeting, 2009. PES’09. IEEE*, 2009, pp. 1–3.
- [17] P. Dondi, D. Bayoumi, C. Haederli, D. Julian, and M. Suter, “Network integration of distributed power generation,” *Journal of power sources*, vol. 106, no. 1-2, pp. 1–9, 2002.
- [18] H. Farhangi, “The path of the smart grid,” *IEEE power and energy magazine*, vol. 8, no. 1, 2010.
- [19] R. H. Lasseter, J. H. Eto, B. Schenkman, J. Stevens, H. Vollkommer, D. Klapp, E. Linton, H. Hurtado, and J. Roy, “Certs microgrid laboratory test bed,” *IEEE Transactions on Power Delivery*, vol. 26, no. 1, pp. 325–332, 2011.
- [20] J. Du, S. Kar, and J. M. Moura, “Distributed convergence verification for Gaussian belief propagation,” *Asilomar Conference on Signals, Systems and Computers (ASILOMAR)*, *arXiv preprint arXiv:1711.09888*, 2017.
- [21] F. Katiraei, R. Iravani, N. Hatziargyriou, and A. Dimeas, “Microgrids management,” *IEEE power and energy magazine*, vol. 6, no. 3, 2008.
- [22] J. Du, S. Ma, Y.-C. Wu, S. Kar, and J. M. Moura, “Convergence analysis of the information matrix in Gaussian belief propagation,” *IEEE International Conference on Acoustics, Speech and Signal Processing (ICASSP)*, *arXiv preprint arXiv:1704.03969*, 2017.
- [23] J. Du, S. Ma, Y.-C. Wu, S. Kar, and J. M. Moura, “Convergence analysis of distributed inference with vector-valued Gaussian belief propagation,” *arXiv preprint arXiv:1611.02010*, 2016.
- [24] J. Du and Y.-C. Wu, “Network-wide distributed carrier frequency offsets estimation and compensation via belief propagation,” *IEEE Transactions on Signal Processing*, vol. 61, no. 23, pp. 5868–5877, 2013.
- [25] J. Du and Y.-C. Wu, “Distributed clock skew and offset estimation in wireless sensor networks: Asynchronous algorithm and convergence analysis,” *IEEE Transactions on Wireless Communications*, vol. 12, no. 11, pp. 5908–5917, 2013.
- [26] J. Du, S. Ma, Y.-C. Wu, and H. V. Poor, “Distributed hybrid power state estimation under PMU sampling phase errors,” *IEEE Transactions on Signal Processing*, vol. 62, no. 16, pp. 4052–4063, 2014.
- [27] L. Chen, N. Li, L. Jiang, and S. H. Low, “Optimal demand response: Problem formulation and deterministic case,” in *Control and optimization methods for electric smart grids*. Springer, 2012, pp. 63–85.
- [28] N. Li, L. Chen, and S. H. Low, “Optimal demand response based on utility maximization in power networks,” in *Power and Energy Society General Meeting, 2011 IEEE*. IEEE, 2011, pp. 1–8.
- [29] J. C. Duchi, S. Shalev-Shwartz, Y. Singer, and A. Tewari, “Composite objective mirror descent,” in *COLT*, 2010, pp. 14–26.
- [30] S. Bubeck, “Introduction to online optimization. princeton university: Lecture notes, 2011.”
- [31] J. Du and Y.-C. Wu, “Fully distributed clock skew and offset estimation in wireless sensor networks,” in *IEEE International Conference on Acoustics, Speech and Signal Processing (ICASSP)*, 2013, pp. 4499–4503.
- [32] S. Barker, A. Mishra, D. Irwin, E. Cecchet, P. Shenoy, and J. Albrecht, “Smart*: An open data set and tools for enabling research in sustainable homes,” *SustKDD, August*, vol. 111, no. 112, p. 108, 2012.
- [33] D. Chen, S. Barker, A. Subbaswamy, D. Irwin, and P. Shenoy, “Non-intrusive occupancy monitoring using smart meters,” in *Proceedings of the 5th ACM Workshop on Embedded Systems For Energy-Efficient Buildings*. ACM, 2013, pp. 1–8.